

Solar cycle signatures in lightning activity

Jaroslav Chum¹, Ronald Langer², Ivana Kolmašová^{1,3}, Ondřej Lhotka¹, Jan Ruzs¹, Igor Strhářský²

¹Institute of Atmospheric Physics of the Czech Academy of Sciences, Prague, 156 00, Czech Republic

²Institute of Experimental Physics, Slovak Academy of Sciences, Košice, 040 01, Slovakia

5 ³Faculty of mathematics and Physics, Charles University, Prague, 180 00, Czech Republic

Correspondence to: Jaroslav Chum (jachu@ufa.cas.cz)

Abstract

10 The cross-correlation between annual lightning frequency and solar activity and the heliospheric magnetic field (HMF) is examined on a global scale using corrected data from the World Wide Lightning Location Network (WWLLN) for the period 2009 to 2022. Relatively large regions with significant cross-correlation coefficients ($p < 0.05$) between the yearly lightning rates and sunspot number (SSN) are found in east Africa, part of South America overlapping with the South Atlantic Anomaly, Indian Ocean and west coast of Australia. The main region that shows a significant correlation between lightning activity and the 15 B_y component of the HMF and the magnetopause reconnection Kan-Lee electric field matches the South Atlantic anomaly quite well. Also shown are areas that show a significant cross-correlation of lightning activity with the El Niño-Southern Oscillation index.

20 Similar areas of significant cross-correlation are obtained if simulated thunder days are used instead of lightning counts. Possible mechanisms leading to the observed correlations and limitations of the current study are discussed. The findings of the present study do not support previous works indicating that cosmic ray intensity is in phase with the global occurrence of lightning, but they do not rule out the role of cosmic rays on lightning ignition in developed thunderclouds and the role of energetic particles precipitating from the magnetosphere on the significant correlation between lightning and B_y component of the HMF (SSN) in the South Atlantic Anomaly.

25 **1 Introduction**

Possible relationship between solar activity and lightning/thunderstorm occurrence frequency has been investigated for many years. Fritz (1878) correlated thunderstorm frequencies with sunspot number (SSN) for the period 1755-1875 and several European and North-American stations without obtaining a conclusive result. A pioneering study on a global scale was made by Brooks (1934), who used data from 22 areas in
30 different parts of the world and found that the cross-correlation coefficients between annual thunderstorm frequency and SSN were mostly positive. The best cross-correlation (0.88) was obtained for Siberia. However, this result was not confirmed by Kleymenova (1967). Brooks (1934) also showed that some cross-correlation coefficients varied considerably over relatively short distances or were relatively low (absolute value less than 0.2), for example in Europe. Other authors studied the cross-correlation between
35 thunderstorms and solar cycle for specific regions. For example, Aniol (1952) investigated the solar influence on thunderstorm frequency in southern Germany over the interval 1881-1950 and found that the cross-correlation coefficients varied significantly for different subintervals. Stringfellow (1974) obtained the cross-correlation coefficient of 0.8 between thunderstorms in Britain and solar cycle over the interval 1930-1973. Pinto Neto et al. (2013a) identified the solar cycle in thunder day data obtained from selected
40 Brazilian cities for the period 1951-2009 and found mostly an anti-phase relation between SSN and thunder day data.

The above mentioned past studies used daily records of audible thunder and did not deal with thunderstorm intensities or actual number of lightning strokes. This limitation can be overcome by using lightning detection networks. Schlegel et al. (2001) calculated the cross-correlation coefficients between
45 various parameters of solar activity and lightning detected in Germany and Austria using lightning detection systems for the period 1992-2000. In Germany, they found a positive cross-correlation coefficients (around 0.8) between lightning and solar activity, but in Austria the results were inconclusive (cross-correlation coefficients close to zero). In addition, Schlegel et al. (2001) showed that cross-correlation coefficients might differ considerably when using lightning counts from those using only number of thunder days as
50 has been done in the past. Number of studies have also documented that lightning activity can be partially modulated on shorter time scale by the solar rotation, the solar wind and the polarity of the heliospheric magnetic field, HMF (Chronis 2009; Owens et al., 2014; Scott et al., 2014; Owens et al., 2015; Miyahara et al., 2018; Chum et al., 2021). Statistical studies by Voiculescu and Usoskin (2012) and Voiculescu et al. (2013) showed that solar activity might impact cloud cover in specific regions rather than globally.

55 The exact mechanism leading to the link between lightning and solar activity is unknown. Some authors believe that clouds, ionospheric potential and lightning activity might be modulated by the intensity of the cosmic ray (CR) flux entering the atmosphere. For example, Markson (1981) showed positive correlation between the ionospheric potential (atmospheric electric field) and CR, which in turn is controlled by solar

activity and HMF; the CR flux is anti-correlated with solar activity (Usoskin et al., 1998). Cosmic rays may
60 influence lightning activity directly by providing secondary energetic particles (electrons) acting as source
of ionization necessary to ignite lightning, a process that is not yet understood in full detail (Dwyer and
Uman, 2014; Shao et al., 2020). The indirect influence is based on the potential role of CR in the modulation
of cloud electrification, cloud condensation nuclei and clouds (Markson 1981; Kristjánsson et al., 2008;
Kirkby 2008; Svensmark et al., 2009). It is reminded that a number of past studies (e.g., Brooks, 1934;
65 Stringfellow, 1974; Schlegel et al., 2001) found mostly positive correlation between solar activity and
lightning, implying a negative correlation with CR, which would reduce the importance of the direct
mechanism/ionization. Solar activity and weather/climate can also be linked through ultraviolet (UV) solar
radiation, which is absorbed in the middle and upper atmosphere and strongly depends on solar activity.
Changes in stratospheric temperature can then affect radiative balance, global circulation and potentially
70 the tropospheric weather (Gray et al., 2010). The exact mechanisms need to be investigated. For example,
the potential role of planetary waves in this top-down mechanism was discussed by Arnold and Robinson
(1998, 2000) and Balachandran et al. (1999). Changes in the global electric circuit (GEC) associated with
the solar activity were discussed by Markson (1978), who put forward an idea that the atmospheric
electricity is affected by changes in column resistance above thunderstorm due to the ionizing radiation
75 modulated by solar activity. This idea was further followed by Markson and Muir (1980) and Markson
(1981) by investigating the relation between solar wind, cosmic rays and ionospheric potential and finding
negative (positive) correlation between solar wind (cosmic rays), respectively. Hale (1979) suggested to
look for effects more directly related to magnetospheric and auroral processes. On the other hand, (Burns
et al., 2008; Lam and Tinsley, 2016) have investigated the atmospheric electric field and associated pressure
80 changes in polar regions and discussed the possible relationship between solar wind, namely the polarity of
the B_y component of the HMF, and tropospheric weather. They hypothesized that changes in the GEC,
specifically through the downward current could affect cloud microphysics, latent heat and cloud formation.
However, further research and verification of this hypothesis is necessary. Voiculescu et al. (2013) showed
that HMF partially affects cloud cover, specifically low cloud cover at mid- and high-latitudes, which could
85 be consistent with HMF – driven changes in GEC, while it is possible that UV changes (a top-down
mechanism) may play a more important role at low latitudes. Considerable attention is paid to the chemical
dynamical coupling caused by energetic particle precipitation (EPP) that includes both energetic electron
precipitation from radiation belt and solar proton events during enhanced geomagnetic and solar activity as
a potential link between solar activity and climate. EPPs cause changes in the chemical composition of the
90 mesosphere and stratosphere, leading to changes in radiative balance and atmospheric temperature (Seppälä
et al., 2009; Anderson et al., 2014; Mironova et al., 2015; Sinhuber et al., 2018). The role of planetary
waves, polar vortex and phase of quasi-biennial oscillation on the effects of EPP on the atmosphere is often

discussed, with inconsistent results so far (Seppälä et al., 2013; Maliniemi et al., 2013, 2016; Salminen et al., 2019). Another hypothesis involving atmospheric waves was put forward by Prikryl et al. (2018), who
95 based on previous statistical studies, suggested that high-speed solar wind streams are together with associated magneto-hydrodynamic waves responsible for enhanced Joule heating in high-latitude thermosphere and ionosphere that in turn generate atmospheric gravity waves that propagate equatorward, may reach the troposphere, lift the air and initiate convection and cloud formation.

The above review of possible coupling mechanisms indicates that further experimental and theoretical
100 studies are needed to evaluate the relative role and validity of different mechanisms that may link solar activity to climate and lightning frequency. The present study investigates the relation between the solar activity (SSN), the B_y , B_z components of the HMF, CR and lightning activity in various regions around the globe using the World Wide Lightning Location Network.

105 **2 Measurement setup and methods**

The near Earth solar wind data and data of solar activity were retrieved from NASA/GSFC's Space Physics Data Facility OMNIWeb service (<https://omniweb.gsfc.nasa.gov/form/>). The solar data are also compared with the CR flux measured by neutron monitor (NM) with the cut-off rigidity of 3.84 GV located on the summit of Lomnický štít (49.195°N, 20.213°E) at an altitude of 2634 m. The NM is filled with BF_3
110 and is of NM-64 type. More information about the NM can be found in Kudela and Langer (2009) and Chum et al. (2020).

Global lightning data are obtained using the World Wide Lightning Location Network (WWLLN), which consists of approximately 70 sensors operating in the frequency range 3-30 kHz that receive electromagnetic signals generated by lightning strokes and propagating in the waveguide between the
115 Earth's surface and the lower ionosphere (Rodger et al., 2004). The WWLLN was selected because of its global coverage and availability for the authors. It should be noted that the optical LIS detector on the satellite observes mainly low latitudes and that the OTD detector with global coverage worked only from 1995 to 2000. The WWLLN lightning counts in $1^\circ \times 1^\circ$ bins are used in this study, but it is also shown that similar results are obtained if larger bins (3° latitude \times 6° longitude) are used. The data available to the
120 authors start in 2009. It should also be noted that the number of WWLLN sensors was substantially lower before 2009, and therefore the detection efficiency was also significantly lower than today. In addition, corrections of detection efficiency (used in this study and described later) are not available before 2009. It is estimated that the current detection efficiency for CG strokes with peak current at least 30 kA is approximately 30% globally (wwlln.net).

125 To investigate the possible dependence of lightning activity on the solar cycle, we applied a cross-
correlation analysis using one-year lightning counts and one-year averages of sunspot number, NM counts,
and B_y , B_z components of HMF in the GSE coordinate system. The one-year values were used to remove
the seasonal dependence of lightning occurrence. The lightning frequency show trends over the 2009-2022
interval. The trend in lightning data is likely caused by increasing network efficiency due to the increasing
130 number of WWLLN sensors. The dependence of the number of detected lightning on the number of
WWLLN sensors was shown by Holzworth et al. (2021). Their Figure 2 shows a clear decrease in the
number of lightning detections before ~2013 due to the lower number of sensors. The applicability of the
WWLLN was also discussed by Virts et al. (2013), who verified that WWLLN lightning climatology is
consistent with in-situ rain observations. Hutchins et al. (2012) introduced a model that account for the
135 uneven global coverage of the WWLLN sensors and variations in the propagation of VLF signals by using
correction coefficients for detection efficiency, currently provided for each hour and $1^\circ \times 1^\circ$ bin. The
correction is especially large for Africa due to the low number of sensors. As will be shown in the "Results"
section, this model (correction) gives relatively high lightning frequency in Africa during the period ~2009-
2013. Therefore, results are also presented for the uncorrected data.

140 To compare time series with different units, scales and relative fluctuations it is useful to standardize
data (normalize by standard deviation after subtracting the mean) using equation (1).

$$a_{norm} = \frac{a - \text{mean}(a)}{\sigma_a}, \quad (1)$$

where a is the analyzed quantity (for example lightning counts, SSN, components of HMF, NM counts etc.)
and σ_a is the standard deviation of its distribution. The cross-correlation coefficients c are

$$145 \quad c = \frac{1}{N-1} \cdot \sum_{i=1}^N \frac{a - \text{mean}(a)}{\sigma_a} \cdot \frac{b - \text{mean}(b)}{\sigma_b} = \frac{1}{N-1} \cdot \sum_{i=1}^N a_{norm} \cdot b_{norm} \cdot \quad (2)$$

The statistical significance is obtained using t-statistics for $N-2$ degrees of freedom and calculated by
the corrcoef function in MATLAB software.

To compare the cross-correlation coefficients obtained for lightning frequency with those for thunder
days (a parameter used in many previous studies), we estimate the thunder days for each bin. The thunder
150 days are estimated as follows. First we calculate the ratio (r_{LAT}) of the area of the $1^\circ \times 1^\circ$ bin (A_{LAT}) to the
thunder detection area (A_T), considering the dependence of the bin area on latitude. The thunder detection
area is computed as $\pi \rho^2$, where $\rho=20$ km, which is the middle value of the thunder audibility range (15 –
25 km) given by Pinto et al. (2013b). The value of ratio r_{LAT} is largest at the equator (9.86) and decreases
with increasing latitude (e.g, it is 5 at the latitude of 50°). Then, to allow some uncertainty in the thunder
155 days (TD), the TD are not determined from a fixed threshold r_{LAT} , but are simulated using logistic function
and summed over the year to get annual values,

$$TD = \sum_{i=1}^M \frac{1}{1+e^{-(N_i-r_{LAT})}} \quad , \quad (3)$$

where N_i is the number of lightning detected in the specific bin on the i -th day and M is the number of days in a year. The logistic function (the individual term summed in equation 3) is very close to zero for $N_i \ll r_{LAT}$ and approaches 1 if $N_i \gg r_{LAT}$. A relatively narrow range of intermediate values of logistic function around $N_i \approx r_{LAT}$ admits some uncertainties.

Potential influence of El Niño–Southern Oscillation (ENSO) on thunderstorm occurrence (Williams et al., 2021; Kolmašová et al., 2022) is also investigated by calculating cross-correlation coefficients between yearly lightning counts (thunder days) and yearly mean of ENSO index. The ENSO index was taken from the NASA webpage [El Niño-Southern Oscillation \(ENSO\) Index | Vital Signs – Ocean Surface Topography from Space \(nasa.gov\)](https://climate.nasa.gov/evidence/details/el-niño-southern-oscillation-ensso-index-vital-signs-ocean-surface-topography-from-space-nasa-gov/).

It should be noted that the solar wind electric field components $E_{zSW} \sim -v_x B_y$ and $E_{ySW} \sim v_x B_z$ are believed to penetrate and add to the internal Earth’s electric field between the ionosphere and ground (Rycroft et al., 2000; Lam and Tinsley, 2016), but since the relative changes in B_y , B_z are much larger than the relative changes in the Earthward solar wind speed v_x , only the dependencies of the Earth’s electric field on B_y or B_z have been often studied (e.g., Burns et al., 2008). We verified that differences between the results obtained for $|v_x|B_y$, $(|v_x|B_z)$ and B_y , (B_z) are negligible.

In addition, the cross-correlation is also computed between lightning counts and magnetopause reconnection electric field (Kan and Lee, 1979). This electric field, namely its perpendicular component, can serve as a proxy for ionospheric electric currents at high latitudes (namely Region 1) during geomagnetic storms, potential across a polar cap (Kan and Lee, 1979; Mannucci et al., 2014) or large scale traveling ionospheric disturbances (LSTID) - waves in the upper atmosphere and ionosphere (Borries et al., 2023). The perpendicular component (related to the magnetic field lines at the magnetopause) of the Kan-Lee electric field (Kan and Lee, 1979) is

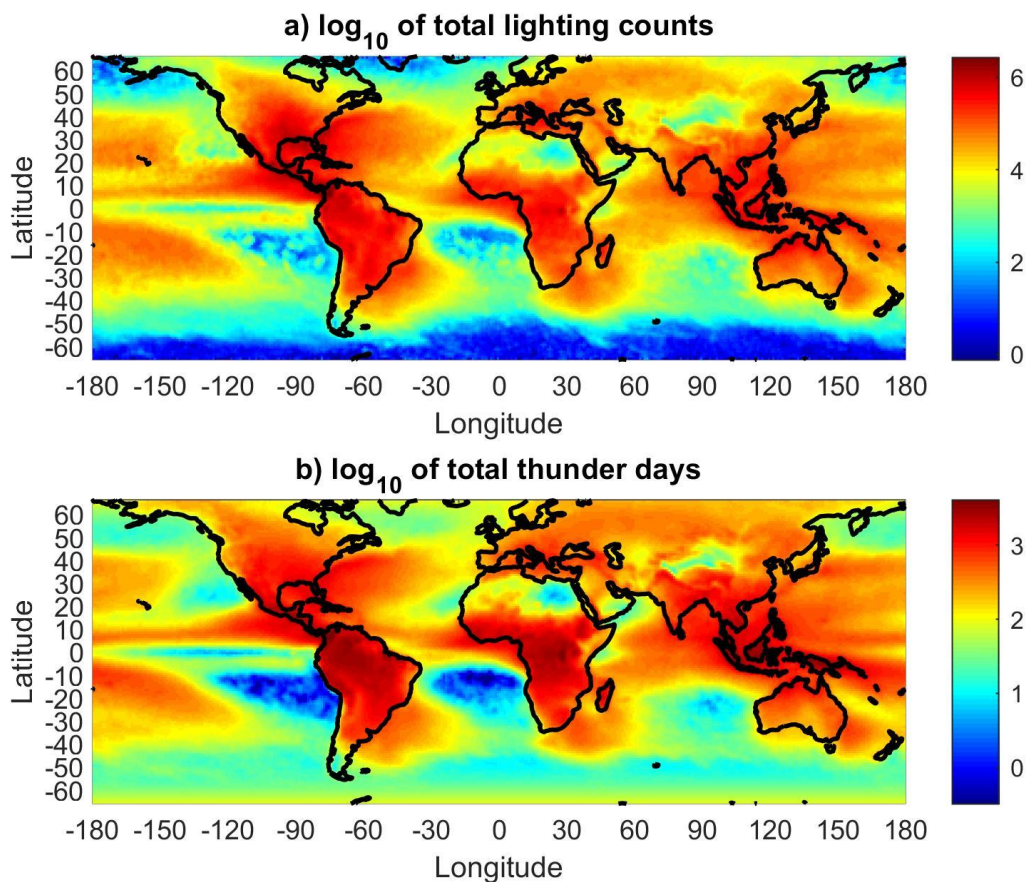
$$E_{perp} = v_x B_T \sin^2(\varphi/2), \quad (4)$$

where B_T is $\sqrt{B_y^2 + B_z^2}$ and φ is a clock angle of the transverse HMF (relative to the z -axis), $\varphi = \text{atan}(B_y/B_z)$. The parallel component of electric field is often neglected in plasma physics because it is believed that it is usually small because of high conductivity along the field line, but Kan and Lee (1979) also pointed out that the parallel component of the reconnection electric field (E_{par}) exists and should not be automatically neglected. The parallel field might accelerate/decelerate particles along the field line and affect their trajectories and precipitation into the atmosphere.

$$E_{par} = v_x B_T \sin(\varphi/2) \cos(\varphi/2). \quad (5)$$

3 Results

190 Figure 1a shows on a world map the global distribution of the total corrected number of lightning strokes recorded by the WWLLN during the analyzed period 2009-2022. The color scale indicates the common logarithm of lightning strokes in each $1^\circ \times 1^\circ$ bin for the latitude range from -66° to 66° . Figure 1b shows, for comparison, the global distribution of the simulated thunder days using Eq. (3). Thunderstorm centers are readily verified in tropical and subtropical regions over the continents, namely Central Africa, South and Central America, East Asia and Indonesia. The continental lightning dominates the oceanic lightning by more than an order of magnitude. Significant numbers of lightning have also been recorded in the Mediterranean. It should be noted that the actual number of lightning is larger because of the limited detection efficiency of the WWLLN, especially for intracloud discharges. Compared to the LIS OTD climatology data set (https://ghrc.nsstc.nasa.gov/lightning/data/data_lis_otd-climatology.html), the WWLLN underestimates the lightning frequency especially in central Africa, where the number of uncorrected detected lightning by WWLLN was about 10 times lower. Therefore, the applied corrections (mentioned in previous section) are largest in Africa as will also be shown later.



205 **Fig. 1** Common logarithm of corrected numbers of all lightning strokes (a) and all thunder days (b) during the analyzed period, 2009-2022.

The cross-correlation coefficients between the yearly SSN and corrected yearly lightning counts are shown in Figure 2a. The cross-correlation coefficients are displayed only for those bins, for which the correlation (anti-correlation) is statistically significant (probability of null hypothesis, $p < 0.05$) and the total number of detected lightning strokes was larger than $2 \cdot 10^3$ for the entire period 2009-2022, which corresponds to an average yearly number of detected lightning larger than ~ 140 in each bin. The same threshold for the required number of detected lightning strokes per bin is used in the following analogous figures. Red color indicates cross-correlation coefficients close to 1, whereas dark blue stands for large negative values of cross-correlation coefficients. It is obvious that lightning activity is in phase – correlates well with solar activity represented by the SSN in central and east Africa, part of South America and the South Atlantic Anomaly region and west coast of Australia.

For comparison with previous works, it is also useful to investigate which regions would exhibit significant cross-correlation coefficients, if thunder day data were used. We use simulated thunder day data obtained from the corrected WWLLN lightning counts by method described in Section 2. The required threshold of $2 \cdot 10^3$ lightning strokes for each bin was modified to $2 \cdot 10^2$ thunder days and the $1^\circ \times 1^\circ$ bins are used. Figure 2b displays the cross-correlation coefficients between yearly sunspot number and simulated yearly thunder days. Although the exact shape of the main regions that show a significant correlation is partly different from those in Figure 2a, which shows the same but using the number of lightning strokes, their approximate locations remain the same: East Africa, part of South America and the west coast of Australia. In addition, there is a relatively large region in East Asia that exhibits significant correlation if thunder days are used.

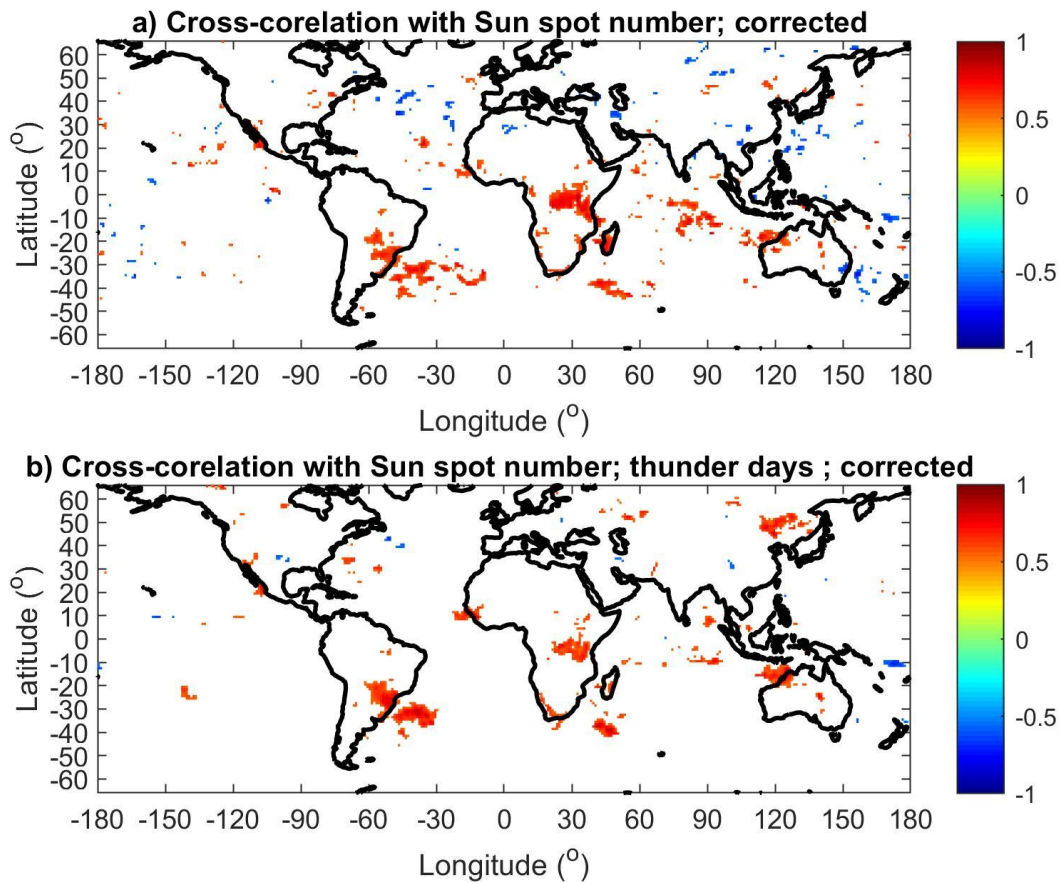


Fig. 2 a) Cross-correlation coefficients between yearly SSN and corrected number of lightning strokes in $1^\circ \times 1^\circ$ bins. b) Cross-correlation coefficients between yearly SSN and simulated yearly thunder days in $1^\circ \times 1^\circ$ bins. Only statistically significant cross-correlation coefficients are displayed ($p < 0.05$).

Figure 3a shows that the cross-correlation coefficients between the yearly SSN and corrected yearly lightning counts in 3° latitude \times 6° longitude bins to demonstrate that the main centers of significant correlation do not change if a different bin size is used (compare Figures 2a and 3a). Figure 3b displays the cross-correlation coefficients between the yearly SSN and uncorrected yearly lightning counts in 3° latitude \times 6° longitude bins to show the effect of correction on WWLLN data. The largest difference is in Africa, where the area with significant correlation is much larger for the uncorrected data. The reason for that is clear from the time series that are presented in Figures 4 and 6.

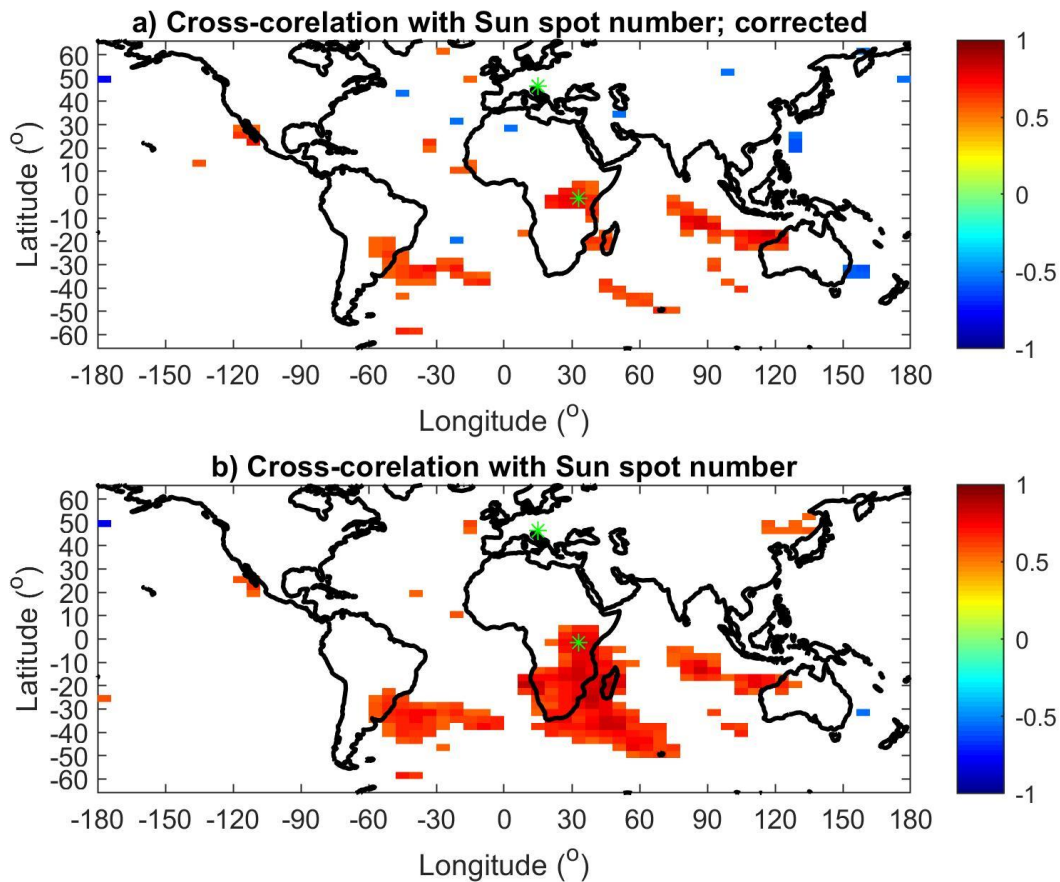


Fig. 3 a) Cross-correlation coefficients between yearly SSN and corrected number of lightning in $3^\circ \times 6^\circ$ (latitude x longitude) bins. b) Cross-correlation coefficients between yearly SSN and uncorrected number of lightning in $3^\circ \times 6^\circ$ (latitude x longitude) bins. Only statistically significant cross-correlation coefficients are displayed ($p < 0.05$). The green asterisks indicate the locations of the selected bins for which time series are shown in Figure 4.

Figure 4 displays the time series of annual SSN (Figure 4a) and annual averages of NM counts measured at Lomnický Štít each minute (Figure 4b). The relative deviations of the NM data from their means are much smaller than for SSN. The mean value and standard deviation for SSN is 47.6 and 38.4, respectively, and for NM counts 27691 and 842. Obviously, the time series of the SSN and NM data are in anti-phase (anti-correlated). This is expected since it is known that the CR flux characterized by NM data is anti-correlated with solar activity (e.g., Usoskin, 1998). An example of the time series of the annual number of lightning strokes for the selected bin in east Africa (latitude from -3° to 0° and longitude from 30° to 36°), in which relatively high and significant cross-correlation coefficient (0.77 for corrected data and 0.90 for corrected smoothed data) was obtained, is shown in Figure 4c. By blue are the uncorrected numbers of

lightning and by red are the corrected numbers using the provided correction coefficients of detection efficiency. The uncorrected and corrected lightning counts significantly differ before 2014. The corrected data are relatively high before 2014, when the solar activity was lower. This is even more remarkable in the surrounding bins and leads to a smaller region of significant correlation, compared to the results obtained for uncorrected data (compare Figures 3a and 3b). On the other hand, in most of the other regions, such as in the selected bin shown in Figure 3d (latitude from 45° to 48° and longitude from 12° to 18°), in which the cross-correlation is statistically insignificant, the differences between corrected and uncorrected lightning counts are small as shows Figure 4d. The selected bins are marked by green asterisks in Figure 3. Figure 5 shows the time series of annual values of B_y , B_z components of HMF, perpendicular and parallel components of Kan-Lee electric field calculated from 1-day values and yearly means of ENSO index. The normalized annual time series of SSN, NM counts and lightning counts for the selected bins are presented in Figure 6.

As discussed in the Introduction, some of the previous studies showed a relation between the polarity (sign) of the HMF components (especially of B_y) and atmospheric electric field at high latitudes and lightning or cloud cover at specific altitudes (Burns et al., 2008; Voiculescu et al., 2013; Owens et al. 2014). First, it is useful to investigate how the individual components of the HMF correlate with the SSN. The cross-correlation coefficients between the used yearly NM data, HMF components, Kan-Lee reconnection electric field and ENSO index are shown in Table 1.

Table 1. Cross-correlation coefficients $C_{SSN,i}$ between yearly SSN and NM, B_y , B_z components of HMF, reconnection electric field, and ENSO index and the corresponding p values.

	NM	B_y	B_z	E_{perp}	E_{par}	ENSO
$C_{SSN,i}$	-0.94	0.34	0.17	0.68	0.28	-0.42
p -value	$<10^{-6}$	0.24	0.55	0.007	0.33	0.14

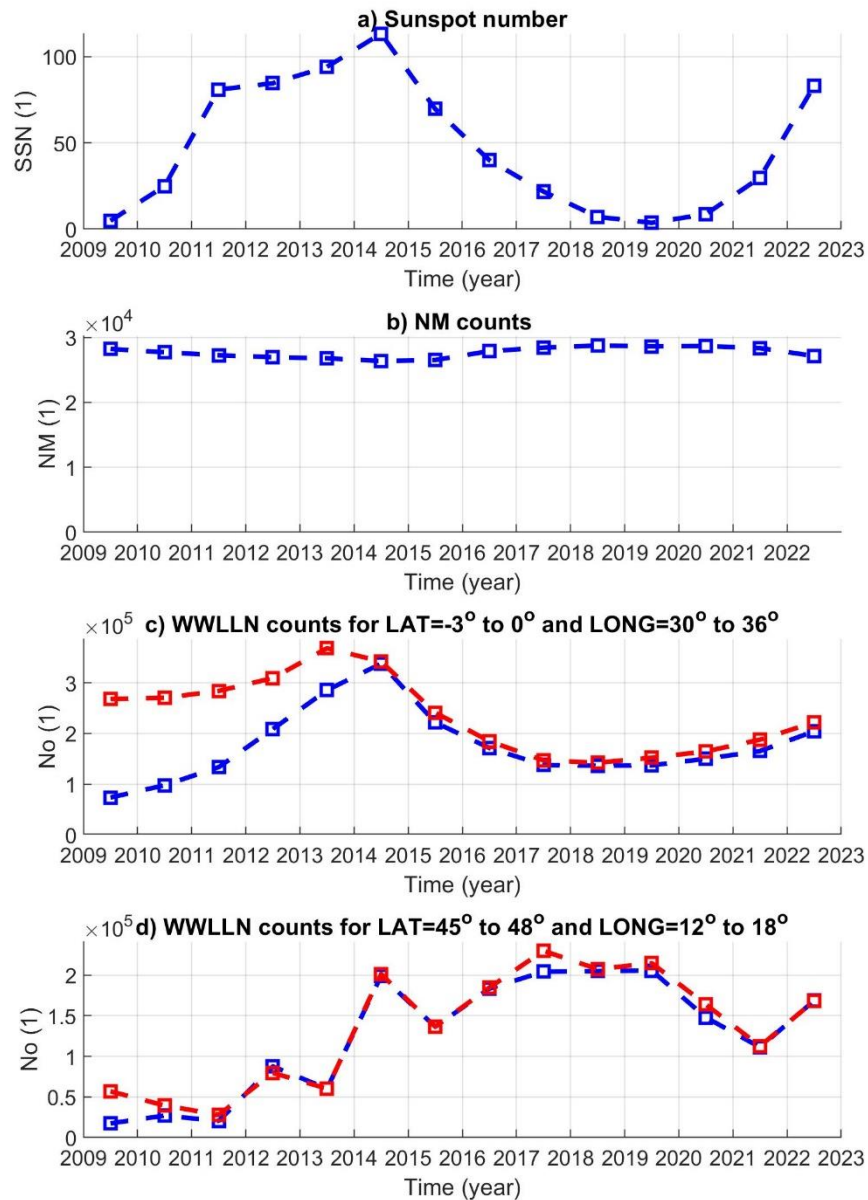
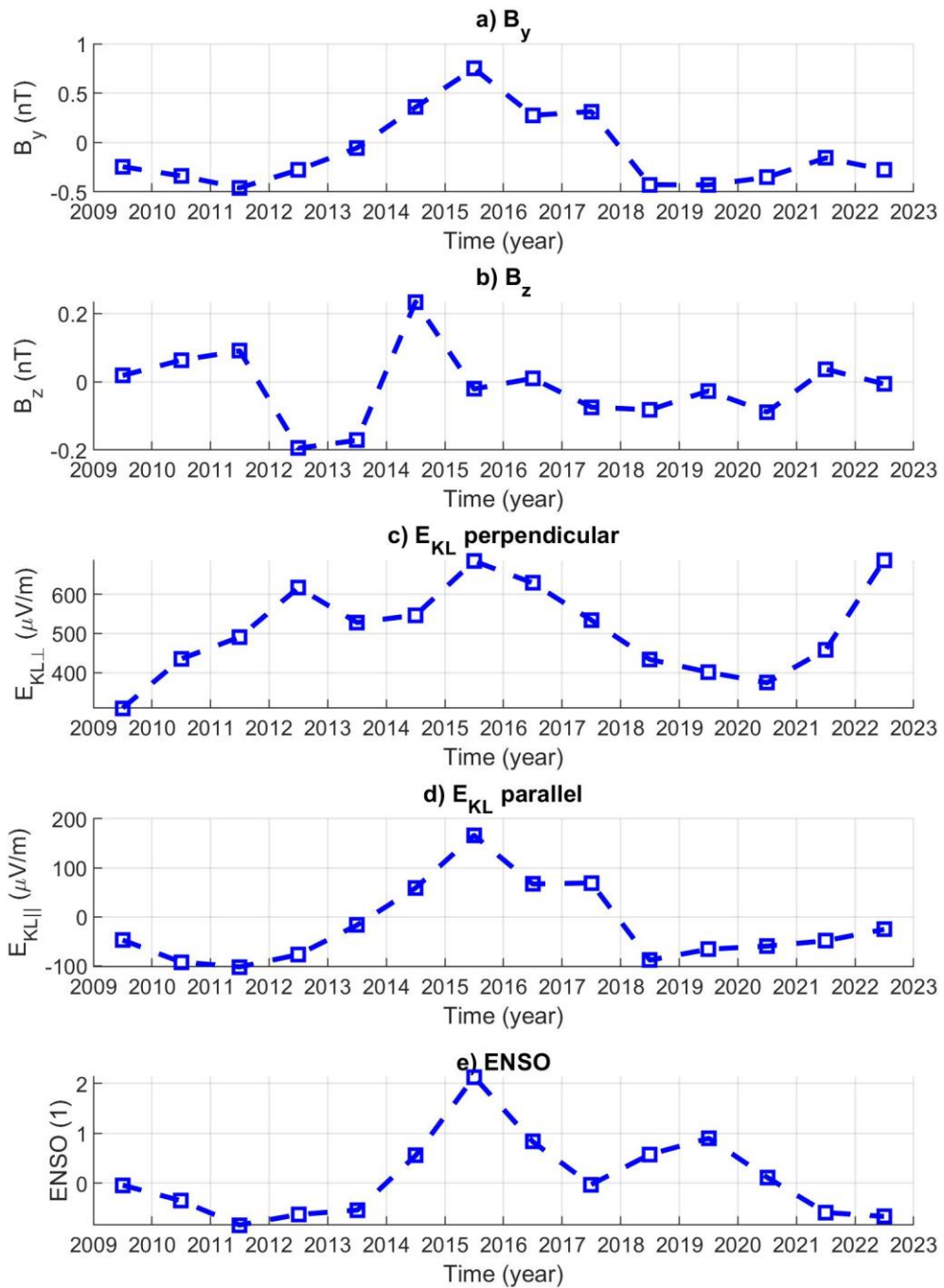


Fig. 4 a) Yearly sunspot number. b) Yearly averages of 1 min NM counts measured at Lomnický Štít. c) 275 Number of detected lightning in the selected bin in which high cross-correlation with SSN was found, latitude from -3° to -0° and longitude from 30° to 36° . d) Number of detected lightning in the selected bin in which significant correlation with SSN was not found, latitude from 45° to 48° and longitude from 12° to 18° . The corrected lightning counts are by red (see text for more details)



280 **Fig. 5** a) Yearly means of B_y (a), B_z (b), perpendicular (c) and parallel (d) component of Kan-Lee electric field calculated from 1-day values and yearly means of ENSO index (e).

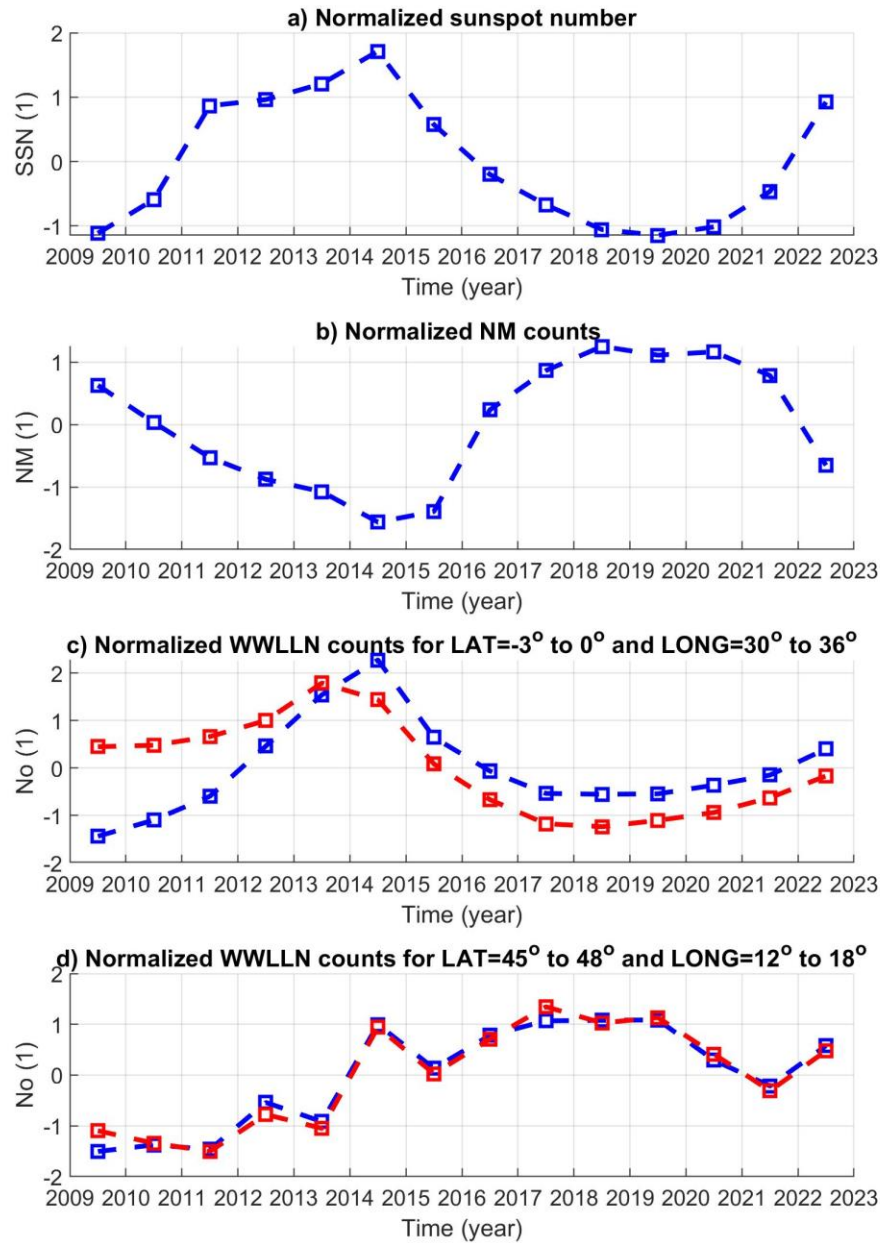


Fig. 6 a) Normalized yearly SSN. b) Normalized yearly NM counts measured at Lomnický Štít. c) Normalized number of lightning in the selected bin in which significant cross-correlation with SSN was found, latitude from -3° to -0° and longitude from 30° to 36° . d) Normalized annual number of lightning strokes in the selected bin in which significant correlation with SSN was not found, latitude from 45° to 48° and longitude from 12° to 18° . Corrected normalized counts are by red, uncorrected by blue.

The NM data are very well anti-correlated (-0.94 , $p < 10^{-6}$) with the SSN, so maps of cross-correlation coefficients between NM and lightning counts is just an opposite (negative) image to the maps shown, e.g.,
 290 in Figure 2. More interesting is a map of cross-correlation coefficients between the B_y , B_z components of the HMF and lightning counts, shown in Figure 7. It is obvious that lightning activity correlates with B_y over south-east part of South America (including South Atlantic) and over smaller regions in Europe, Asia and North America (Fig. 7a). On the other hand, only few relatively small regions show significant cross-correlation between lightning counts and B_z (Fig. 7b). A comparison of Figure 2a and Figure 7a reveals that
 295 main difference between maps for the cross-correlation with the SSN and the B_y component is that significant cross-correlation with B_y is not found in Africa. Figure 8 shows that similar results are obtained if thunder days, instead of lightning counts, are used. In addition, regions that show anti-correlation (e.g., in Colombia and Venezuela) are identified in Figure 8a. Again, practically no significant cross-correlation is found with the B_z component (Figure 8b).

300

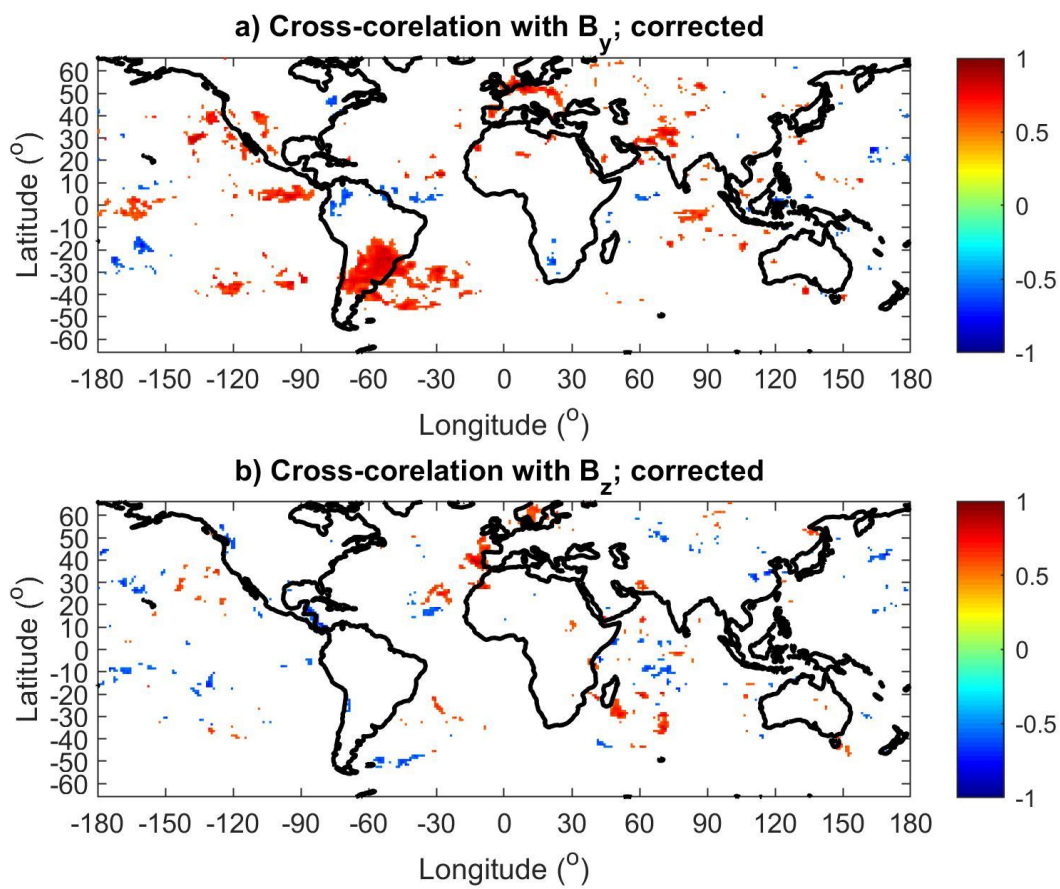


Fig. 7 a) Cross-correlation coefficient between yearly B_y component of HMF and corrected lightning counts in $1^\circ \times 1^\circ$ bins. b) Cross-correlation coefficient between yearly B_z component of HMF and corrected

lightning counts in $1^\circ \times 1^\circ$ bins. Only statistically significant cross-correlation coefficients are displayed ($p < 0.05$).

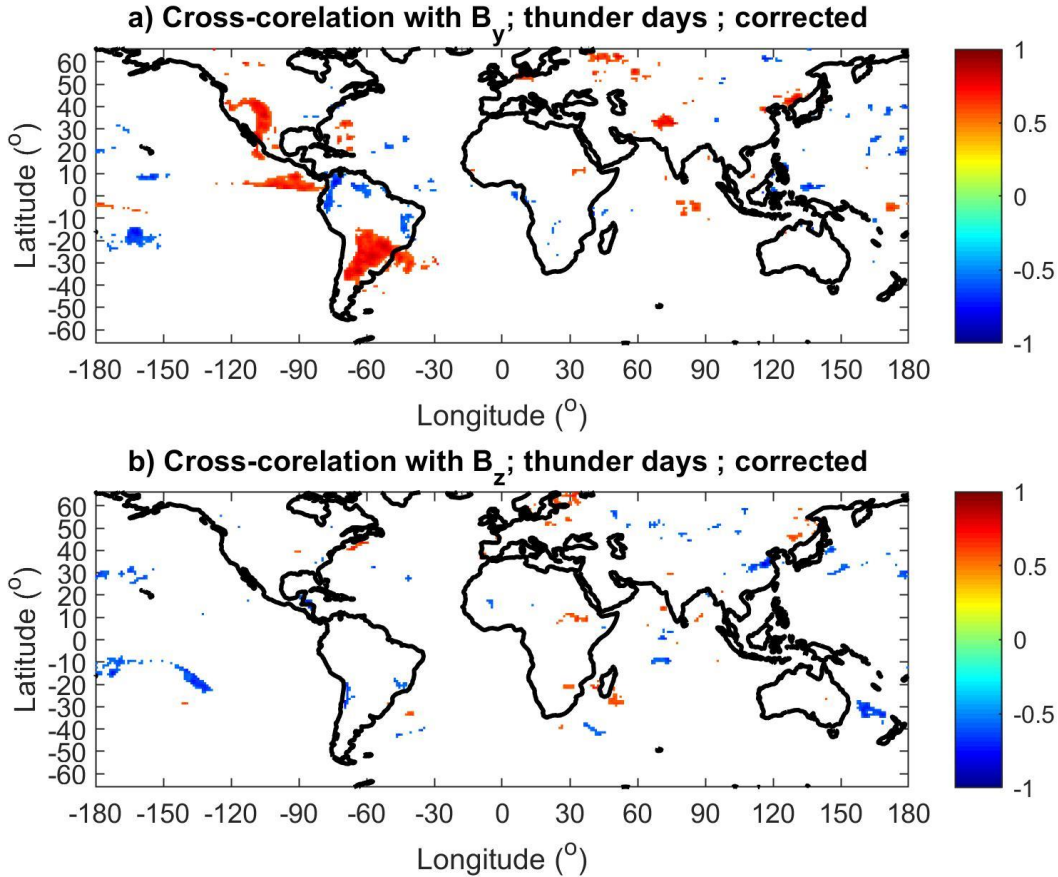
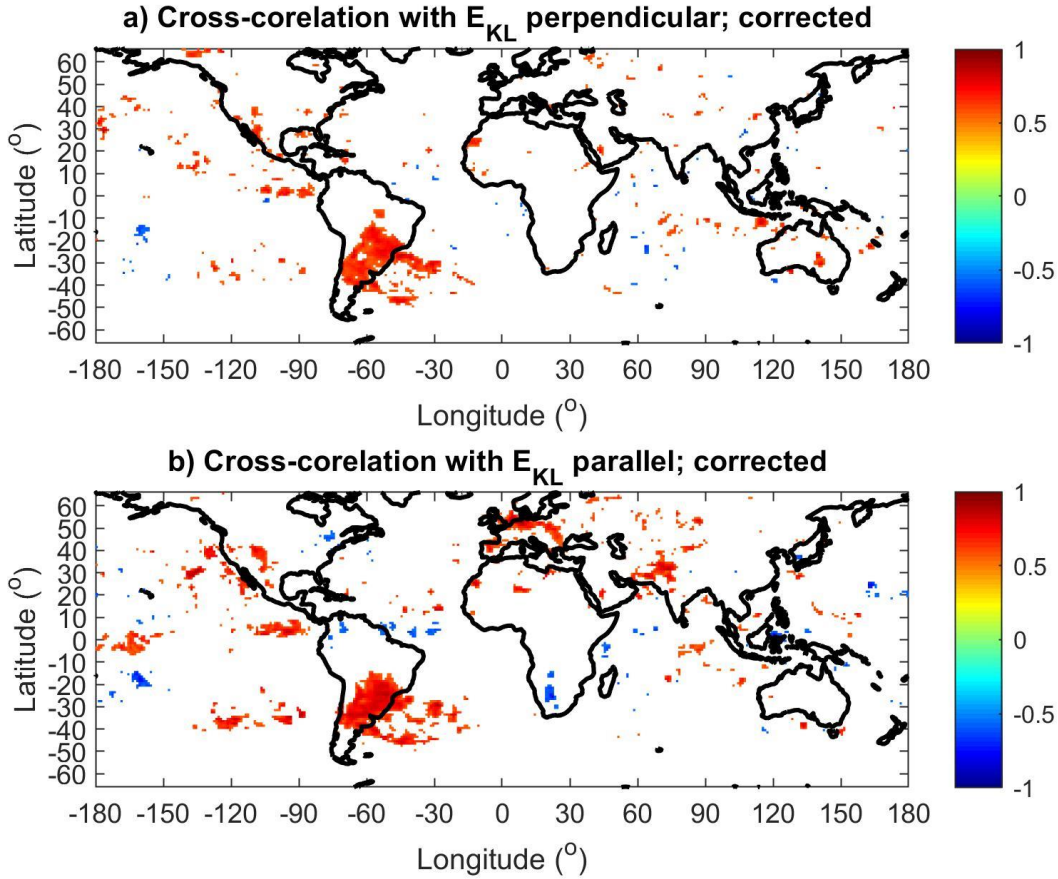


Fig. 8 a) Cross-correlation coefficient between yearly B_y component of HMF and corrected lightning counts in $1^\circ \times 1^\circ$ bins. b) Cross-correlation coefficient between yearly B_z component of HMF and corrected lightning counts in $1^\circ \times 1^\circ$ bins. Only statistically significant cross-correlation coefficients are displayed ($p < 0.05$).

The cross-correlation coefficients between the corrected lightning counts and magnetopause reconnection electric field (Kan-Lee) are shown in Figure 9. Significant and large values (up to about 0.85) are obtained in the south-east part of South America both for the perpendicular (Figure 9a) and parallel component (Figure 9b). The map of cross-correlation coefficients, mainly for the parallel component of the Kan-Lee electric field, is very similar to the map for cross-correlation with B_y (compare Figures 7a and 9b). It is actually not surprising because $|B_y|$ is usually larger than $|B_z|$. Therefore $B_T \approx |B_y|$ in the first approximation, and since, in addition, the absolute value of the term $\sin(\varphi/2)\cos(\varphi/2)$ peaks for $B_z=0$

320 ($|\varphi|/2=45^\circ$), the fluctuations of the parallel component of the Kan-Lee electric field defined by equation (5) roughly follow the fluctuations of B_y , including the sign. Similar results are obtained if thunder days are used.



325 **Fig. 9** a) Cross-correlation coefficient between reconnection Kan-Lee electric field (perpendicular component) and corrected lightning counts in $1^\circ \times 1^\circ$ bins. b) Cross-correlation coefficient between reconnection Kan-Lee electric field (parallel component) and corrected lightning counts in $1^\circ \times 1^\circ$ bins. Only statistically significant cross-correlation coefficients are displayed ($p < 0.05$).

Williams et al. (2021) and Kolmašová et al. (2022) showed that ENSO can influence the lightning
 330 occurrence. Figure 10 shows maps of significant ($p < 0.05$) cross-correlation coefficients between the ENSO index and corrected lightning counts (Figure 10a) and simulated thunder days (Figure 10b). The results for lightning counts and thunder days are qualitatively similar, but regions of negative (anti-phase) correlation are larger if thunder days are used, especially in equatorial Amerika, equatorial Atlantic and Indonesia. Negative cross-correlations are also identified in South Africa. Positive correlations are found in South
 335 America, east Pacific, but also partly in Europe, Mediterranean and western part of the USA.

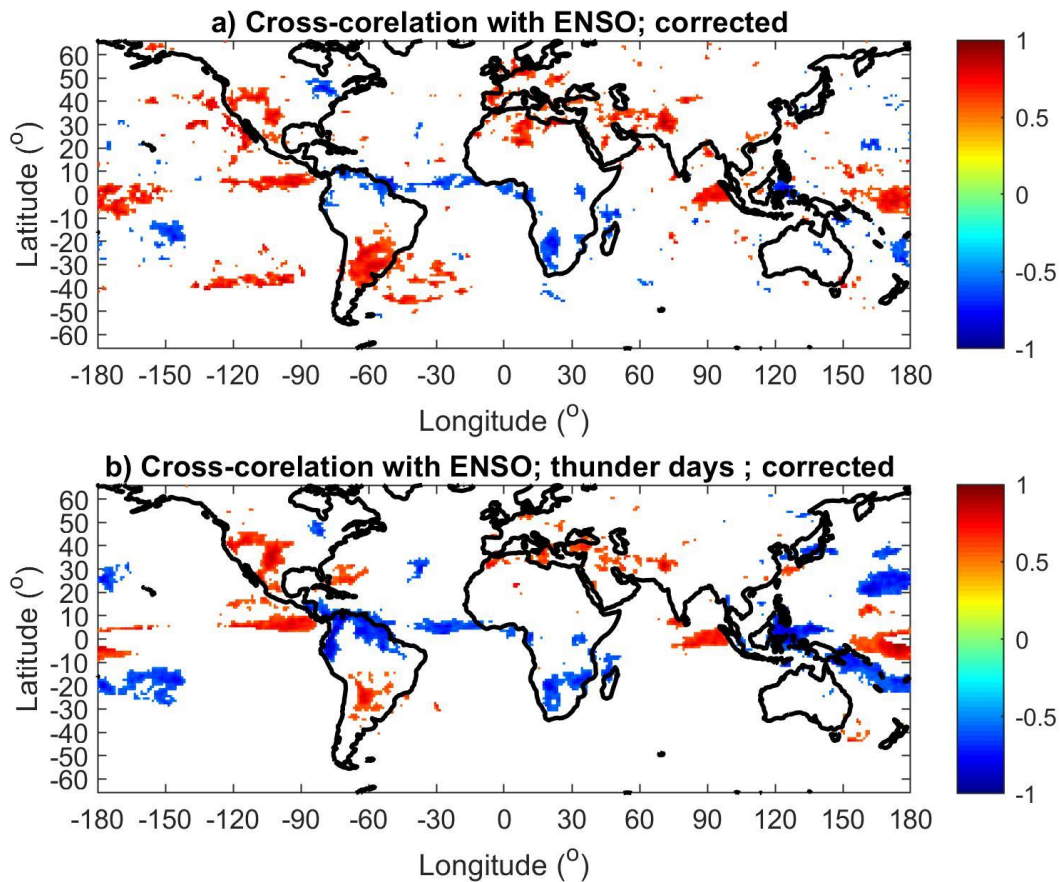


Fig. 10 a) Cross-correlation coefficients between yearly mean of ENSO index and corrected number of lightning strokes in $1^\circ \times 1^\circ$ bins. b) Cross-correlation coefficients between yearly mean of ENSO index and simulated thunder days in $1^\circ \times 1^\circ$ bins. Only statistically significant cross-correlation coefficients are displayed ($p < 0.05$).

4. Discussion and Conclusions

The presented maps show that significant cross-correlation coefficients ($p < 0.05$) between solar activity represented by the SSN and lightning are observed in central and east Africa, south-east part of South America, including part of South Atlantic, and west coast of Australia and part of Indian Ocean for the period 2009-2022. It should be noted that the regions of significant correlation do not include most of the typical wet rain forest areas, the Amazon basin in America, west part of Congo basin in Africa and south-east Asia and Indonesia. The total area showing significant cross-correlation is relatively small and a partial/random coincidence cannot be entirely ruled out. Therefore, we discuss possible mechanisms or connections below. In this respect, it should also be noted that especially small and randomly distributed

are the areas with significant cross-correlation between lightning activity and the B_z component of the HMF. In this latter case, the random coincidence is quite probable.

Mutai and Ward (2000) found that rain events in east Africa are associated with the Madden Julian oscillation (MJO) in the Indian ocean. The rains in Africa are usually associated with thunderstorms. Kozlov
355 et al. (2023) found that the ionospheric potential follows the MJO phase. We note that both east Africa and the Indian ocean show significant correlation with the SSN. It was also shown that the intensities of rain events in east Africa depend on the phase of the ENSO (Ogallo, 1988; Nicholson and Kim, 1997). However, our analysis does not show significant cross-correlation between the lightning activity and ENSO index in
360 east Africa (Figure 10). Pinto et al., (2013b) found that an increase of thunderstorm activity around Rio de Janeiro occurs simultaneously with a positive anomaly of the South Atlantic sea surface temperature and La Niña. This is partly confirmed by our study, however, the regions that show significant anti-phase correlation with the ENSO index are rather the equatorial regions of South America (Figure 10). Williams et al. (2021), based on Schumann resonance measurements, found that the global lightning activity
365 increased in the transition phase to El Niño. It should be noted that strong El Niño occurred in 2014-2015, which coincides with a maximum of the solar cycle 24. On the other hand, there were two relatively weak El Niño phases during the 2009-2010 and 2018-2019 solar minima, but the 2009-2010 El Niño in particular was very short and difficult to recognize in the annual averages of the ENSO index (Fig. 5e). Nevertheless, it should be noted that the cross-correlation maps of lightning activity with the SNN (Figure 2) and ENSO
370 index (Figure 10) look different; in the latter case, more regions with significant anti-phase relation can be found.

It is probable that regional climatic differences are responsible for the observed patterns in the maps of significant correlation (anti-correlation) with the SSN, but the exact mechanism is not clear and needs further investigation. Barriopedro et al. (2008) found that the 11-year solar cycle (represented by the SSN)
375 modulates atmospheric blocking in mid-latitudes of the northern hemisphere. Proposed underlying physical mechanisms are related to heating in the stratosphere by UV radiation (Gray et al. 2016). Changes in blocking frequency, persistence and locations affect atmospheric circulation, which is a main factor modulating surface weather and climate patterns at mid-latitudes (Masato et al. 2012). However, the observed relationships between SSN and atmospheric circulation in the troposphere were significant only
380 in boreal winter, when the lightning activity is relatively low compared to summer, and cannot explain the relation based on annual data.

Pinto et al. (2013a), using audible thunder data from 1951 to 2009, found a solar cycle signature in thunderstorm activity in several Brazilian cities, with significant anti-phase relation with the SSN for three out of seven cities. This is not confirmed in the current study that covers period from 2009 to 2022. In
385 contrast, significant in-phase relation was found in the south part of Brazil. It should be noted that the anti-

correlation is consistent with the idea of Markson (1981), who suggested that thunderstorm activity is in-phase with cosmic rays and in anti-phase with solar activity. According to our study, however, cosmic rays are uncorrelated with lightning activity over most of the globe. More important are probably weather conditions leading to thunderstorm formation. This does not rule out the possibility that cosmic rays play a
390 role in igniting individual lightning strikes in already developed thunderclouds (Shao et al., 2020).

Comparison of the maps obtained using lightning counts and simulated thunder days shows that although the patterns of areas with significant cross-correlation with the SSN are not exactly identical, they are not very different and the approximate location of the major centers remains the same. Unlike Schlegel et al. (2001), we have not found significant correlation between the lightning frequency in Germany and SSN.
395 On the other hand, a significant correlation was found between lightning frequency in Germany and the B_y component of the HMF and the reconnection Kan-Lee electric field (Figure 7a, Figure 9b).

An important and interesting result of the present study is that the region of significant correlation between lightning activity and the B_y component of the HMF and the reconnection Kan-Lee electric field coincides with the region of the South Atlantic Anomaly (SAA). This result is valid for both lightning
400 counts and thunder days. It is known that a relatively large number of energetic particles precipitate from the magnetosphere into the atmosphere due to the decreased strength of the magnetic field in the SAA region, especially during interaction of solar wind with the Earth's magnetosphere. For example, Sauvaud et al. (2008) showed, using measurements onboard DEMETER satellite, a large flux of 200 keV precipitating (loss-cone) electrons when the satellite was inside the SAA. On the other hand, east Africa
405 does not exhibit correlation with the B_y component of the HMF and the reconnection Kan-Lee electric field. Therefore, it cannot be excluded that different mechanisms are responsible for the significant correlation between the SSN and lightning activity in the SAA region and in east Africa, where the precipitation of energetic particles from the magnetosphere is unlikely. Further studies are needed to verify, if energetic particles precipitating from the magnetosphere are indeed responsible for the significant correlation
410 between lightning activity and Kan-Lee electric field (B_y component of the HMF) in the SAA region. The energy spectrum of precipitating particles, their effect on the ionization, electric conductivity, chemical compositions at different heights, radiative balance, cloud cover and cloud charging need to be analyzed.

It should also be noted that precipitating particles and solar x-rays, which are usually stronger during solar maximum, enhance the ionization in the bottom ionosphere and upper mesosphere, lowering the
415 reflection height from which the very low frequency and extra low frequency electromagnetic waves are reflected (Sátori et al., 2005; Bozóki et al., 2021). Changes in properties in the upper part of the Earth-Ionosphere waveguide can thus bias/affect the detection efficiency of the WWLLN.

Another limitation of the current study is a relatively short analyzed period 2009-2022, which only covers solar cycle 24 and the beginning of cycle 25. In addition, the time series variations of the B_y

420 component of the HMF and ENSO index look very similar before 2017 (Figures 5a and 5e). It is not clear
whether the obtained patterns of significant cross-correlation coefficients between lightning and solar
activity or HMF are also valid for other time periods/solar cycles. Some previous studies based on thunder
days, such as that of Aniol (1952) suggest that the cross-correlation coefficients between thunder days in
Germany and solar activity vary with time. Similarly, Chum et al. (2021) identified a period of solar rotation
425 in lightning data in Central Europe at the period 2016-2019 (lightning was more probable if the HMF was
oriented toward the Sun). However, extending their study to a longer time interval reveals that the period
observed in lightning data and period of solar rotation (period of HMF polarity) are generally asynchronous,
although they may be close together. Further studies, based on longer time intervals, are needed to verify
the results presented in this study.

430

Abbreviations

CR: Cosmic rays; ENSO: El Niño–Southern Oscillation; HMF: Heliospheric magnetic field; LS:
Lomnický štít; MJO: Madden Julian oscillation; NM: Neutron monitor; WWLLN: World-wide
lightning location network; SAA: South Atlantic anomaly; SSN: sunspot number

Data Availability

WWLLN archival data are copyrighted by the University of Washington and are available to the public at
nominal cost. The Solar activity and HMF data can be found at NASA/GSFC's Space Physics Data
Facility's OMNIWeb (<https://omniweb.gsfc.nasa.gov/>).

The NM data can be downloaded from <http://data.space.saske.sk/status/> (access is provided by R. Langer,

440 langer@saske.sk, on request).

Author Contributions

JC designed and wrote the paper and performed most of the analysis. RL and IS are responsible for and
provided the SCR data. IK provided the lightning data and contributed to the discussion. OL and JR

445 contributed to the discussion. All authors read and approved the submitted version.

Competing Interest

The authors declare that they have no conflict of interest.

Acknowledgments

450 We are grateful to Samuel Štefánik for maintaining the measurements on Lomnický Štít. The authors thank E. Williams and an anonymous reviewer for valuable comments that greatly improved the manuscript.

Funding

Support under the grant SAV-23-02 by the Czech Academy Sciences is acknowledged. The work of IK
455 was supported by the Czech Science Foundation grant 23-06430S.

References

- Andersson, M. E., Verronen, P. T., Rodger, C. J., Clilverd, M. A., and Seppälä, A. (2014), Missing driver in the Sun-Earth connection from energetic electron precipitation impacts mesospheric ozone, *Nat. Commun.*, 5, 5197, <https://doi.org/10.1038/ncomms6197>
- 460 Aniol, R. (1952). Schwankungen der Gewitterhäufigkeit in Süddeutschland. *Meteorologische Rundschau* 3 (4), 55–56.
- Arnold, N.F., Robinson, T.R. (1998). Solar cycle changes to planetary wave propagation and their influence on the middle atmosphere circulation. *Annales de Geophysique* 16, 69–76.
- 465 Arnold, N.F., Robinson, T.R. (2000). Amplification of the influence of solar flux variations on the middle atmosphere by planetary waves. *Space Science Reviews* 94 (1–2), 279–286.
- Balachandran, N.K., Rind, D., Lonergan, P., Shindell, D.T. (1999). Effects of solar cycle variability on the lower stratosphere and the troposphere. *Journal of Geophysical Research* 104, 27,321–27,339.
- Barriopedro, D., García-Herrera, R., Huth, R. (2008). Solar modulation of Northern Hemisphere winter
470 blocking. *J. Geophys. Res.* 113, D14118. doi: 10.1029/2008JD009789
- Borries, C., Ferreira, A.A., Nykiel, G. et al. (2023), A new index for statistical analyses and prediction of traveling ionospheric disturbances. *J. Atmos. Solar-Terrestrial Phys.*, 247, doi: <https://doi.org/10.1016/j.jastp.2023.106069>
- Bozóki T, Sători G, Williams E, Mironova I, Steinbach P, Bland EC, Koloskov A, Yampolski YM, Budanov OV, Neska M, Sinha AK, Rawat R, Sato M, Beggan CD, Toledo-Redondo S, Liu Y and Boldi R (2021) Solar Cycle-Modulated Deformation of the Earth–Ionosphere Cavity. *Front. Earth Sci.* 9:689127, doi: 10.3389/feart.2021.689127
- Brooks, C.E.P., 1934. The variation of the annual frequency of thunderstorms in relation to sunspots. *Quarterly Journal of the Royal Meteorological Society* 60, 153–165.
- 480 Burns, G. B., Tinsley, B. A., French, W. J. R., Troshichev, O. A., and Frank-Kamenetsky, A. V. (2008). Atmospheric Circuit Influences on Ground-Level Pressure in the Antarctic and Arctic. *J. Geophys. Res.* 113, D15112. doi:10.1029/2007JD009618

- Chronis, T. G. (2009), Investigating possible links between incoming cosmic ray fluxes and lightning activity over the United States, *J. Clim.*, 22, 5748–5754, doi:10.1175/2009JCLI2912.1.
- 485 Chum, J., Langer, R., Baše, J., Kollárik, M., Strhárský, I., Diendorfer, G., and Rusz, J. (2020), Significant enhancements of secondary cosmic rays and electric field at the high mountain peak of Lomnický Štít in High Tatras during thunderstorms, *Earth, Planets and Space*, 72:28, <https://doi.org/10.1186/s40623-020-01155-9>
- 490 Chum, J., Kollárik, M., Kolmašová, I., Langer, R., Rusz, J., Saxonbergová, D. and Strhárský, I. (2021), Influence of Solar Wind on Secondary Cosmic Rays and Atmospheric Electricity. *Front. Earth Sci.* 9:671801. <https://doi.org/10.3389/feart.2021.671801>
- Dwyer, J. R., and Uman, M. A. (2014). The Physics of Lightning. *Phys. Rep.* 534 (4), 147–241. doi:10.1016/j.physrep.2013.09.004
- 495 Fritz, H., 1878. Die wichtigsten periodischen Erscheinungen der Meteorologie und Kosmologie. In: Natuurkundige Verhandelingen van de Hollandsche Maatschappij der Wetenschappen te Haarlem, Deel III, Haarlem
- Gosling, J. T., and Pizzo, V. J. (1999). Formation and Evolution of Corotating Interaction Regions and Their Three Dimensional Structure. *Space Sci. Rev.* 89, 21–52. doi:10.1023/A:100529171190010.1007/978-94-017-1179-1_3
- 500 Gray, L. J., Beer, J., Geller, M., Haigh, D. J., Lockwood, M., Matthes, K., et al. (2010). Solar Influences on Climate. *Rev. Geophys.* 48, RG4001. doi:10.1029/2009RG000282
- Gray, L.J., Woollings, T.J., Andrews, M. and Knight, J. (2016), Eleven-year solar cycle signal in the NAO and Atlantic/European blocking. *Q.J.R. Meteorol. Soc.*, 142, 1890-1903. doi: 10.1002/qj.2782
- 505 Hale, L. Solar modulation of atmospheric electrification and the Sun–weather relationship. *Nature* 278, 373 (1979). <https://doi.org/10.1038/278373a0>
- Holzworth, R. H., Brundell, J. B., McCarthy, M. P., Jacobson, A. R., Rodger, C. J., & Anderson, T. S. (2021). Lightning in the Arctic. *Geophysical Research Letters*, 48, e2020GL091366. <https://doi.org/10.1029/2020GL091366>
- 510 Hutchins, M. L., R. H. Holzworth, J. B. Brundell, and C. J. Rodger (2012), Relative detection efficiency of the World Wide Lightning Location Network, *Radio Sci.*, 47, RS6005, doi:10.1029/2012RS005049.
- Kan, J.R., Lee, L.C. (1979). Energy coupling function and solar wind magnetosphere dynamo. *Geophys. Res. Lett.* 6(7), 577–580, <http://dx.doi.org/10.1029/GL006i007p00577>.
- Kirkby, J. (2008). Cosmic Rays and Climate. *Surv. Geophys.* 28, 333–375. doi:10.1007/s10712-008-9030-610.1007/s10712-008-9030-6
- 515 Kleymenova, E. P. (1967), On the variation of the thunderstorm activity in the solar cycle, *Glav. Uprav. Gidromet. Scuzb., Met. Gidr.* 8, 64–68 (in Russian).

- Kolmašová, I., Santolík, O., Rosická, K. (2022), Lightning activity in northern Europe during a stormy winter: disruptions of weather patterns originating in global climate phenomena, *Atmos. Chem. Phys.*, 22, 5, 3379-3389, <https://doi.org/10.5194/acp-22-3379-2022>
- 520 Kottek, M., Grieser, J., Beck, C., et al (2006). World Map of the Köppen-Geiger climate classification updated. *Meteorologische Zeitschrift* 15, 259–263. doi: 10.1127/0941-2948/2006/0130
- Kozlov, A. V., Slyunyaev, N. N., Ilin, N. V., Sarafanov, F. G., Frank-Kamenetsky, A.V. (2023), The effect of the Madden–Julian Oscillation on the global electric circuit, *Atmospheric Research*, 284, 106585, <https://doi.org/10.1016/j.atmosres.2022.106585>.
- 525 Kristjánsson, J. E., Stjern, C.W., Stordal, F., Fjæraa, A. M., Myhre, G., and Jónasson, K. (2008). Cosmic Rays, Cloud Condensation Nuclei and Clouds – a Reassessment Using MODIS Data. *Atmos. Chem. Phys.* 8 (24), 7373–7387. doi:10.5194/acp-8-7373-2008
- Kudela, K., Langer, R. (2009). Cosmic ray measurements in high Tatra mountains: 1957–2007. *Advances in Space Research*, 44(10), 1166–1172, <https://doi.org/10.1016/j.asr.2008.11.028>
- 530 Lam, M. M., and Tinsley, B. A. (2016). Solar Wind-Atmospheric Electricity-Cloud Microphysics Connections to Weather and Climate. *J. Atmos. Solar-Terrestrial Phys.* 149, 277–290. doi:10.1016/j.jastp.2015.10.019
- Maliniemi, V., Asikainen, T., Mursula, K. & Seppälä, A. (2013). QBO dependent relation between electron precipitation and wintertime surface temperature, *J. Geophys. Res. Atmos.*, 118, 6302-6310
- 535 Maliniemi, V., Asikainen, T. & Mursula, K. (2016), Effect of geomagnetic activity on the northern annular mode: QBO dependence and the Holton-Tan relationship, *J. Geophys. Res. Atmos.*, 121
- Mannucci, A.J., Crowley, G., Tsurutani, B.T., Verkhoglyadova, O.P., Komjathy, A., Stephens, P., 2014. Interplanetary magnetic field By control of prompt total electron content increases during superstorms. *J. Atmos. Sol. Terr. Phys.* 115–116, 7–16. <http://dx.doi.org/10.1016/j.jastp.2014.01.001>.
- 540 Markson, R. (1978), Solar modulation of atmospheric electrification and possible implications for the Sun–weather relationship. *Nature* 273, 103–109. <https://doi.org/10.1038/273103a0>
- Markson, R. (1981), Modulation of the Earth's electric field by cosmic radiation. *Nature* 291, 304–308. <https://doi.org/10.1038/291304a0>
- Markson and Muir (1980), Solar wind control of the Earth's electric field, *Science* 208, 979-990, DOI: 10.1126/science.208.4447.979
- 545 Masato, G., Hoskins, B.J. and Woollings, T.J. (2012). Wave-breaking characteristics of midlatitude blocking. *Q.J.R. Meteorol. Soc.*, 138: 1285-1296. doi: 10.1002/qj.990
- Mironova, I.A., Aplin, K.L., Arnold, F. et al. (2015). Energetic Particle Influence on the Earth's Atmosphere. *Space Sci Rev*, 194, 1–96, <https://doi.org/10.1007/s11214-015-0185-4>

- 550 Miyahara, H. and Kataoka, R. and Mikami, T. and Zaiki, M. and Hirano, J. and Yoshimura, M. and Aono, Y. and Iwahashi, K. (2018), Solar rotational cycle in lightning activity in Japan during the 18-19th centuries, *Ann. Geophys.*, *36*, 633–640, <https://doi.org/10.5194/angeo-36-633-2018>
- Mutai, C. and Ward, M. (2000), East African Rain fall and the Tropical Circulation/Convection on Intraseasonal to Interannual Timescales, *Journal of Climate*, *13*, (22), 3915–3939.
- 555 Nicholson and J. Kim (1997), The relationship of the El Niño–Southern Oscillation to African rainfall. *Int. J. Climatol.*, *17*, 117–135.
- Ogallo, L. J. (1988), Relationship between seasonal rainfall in East Africa and Southern Oscillation. *J. Climatol.*, *8*, 34–43.
- Owens, M., Scott, C., Lockwood, M., Barnard, L., Harrison, R., Nicoll, K., Watt, C., and Bennett, A.
- 560 (2014), Modulation of UK lightning by heliospheric magnetic field polarity, *Environ. Res. Lett.*, *9*(11), 115009, <https://doi.org/10.1088/1748-9326/9/11/115009>.
- Owens, M. J., Scott, C. J., Bennett, A. J., Thomas, S. R., Lockwood, M., Harrison, R. G., and Lam, M. M. (2015), Lightning as a space-weather hazard: UK thunderstorm activity modulated by the passage of the heliospheric current sheet, *Geophys. Res. Lett.*, *42*, 9624–9632, <https://doi.org/10.1002/2015GL066802>.
- 565 Pinto Neto, O., Pinto, I. R. C. A., and Pinto, O. (2013a), The relationship between thunderstorm and solar activity for Brazil from 1951 to 2009, *J. Atmos. Sol. Terr. Phys.*, *98*, 12–21, doi:10.1016/j.jastp.2013.03.010.
- Pinto, O., I. R. C. A. Pinto, and M. A. S. Ferro (2013b), A study of the long-term variability of thunderstorm days in southeast Brazil. *J. Geophys. Res. Atmos.*, *118*, 5231–5246, <https://doi.org/10.1002/jgrd.50282>.
- 570 Prikryl, P., Bruntz, R., Tsukijihara, T., Iwao, K., Muldrew, D. B., Rušin, V., Rybanský, M., Turňa, M., and Šťastný, P. (2018), Tropospheric weather influenced by solar wind through atmospheric vertical coupling downward control, *J. Atmos. Sol. Terr. Phys.*, *171*, 94–110, <https://doi.org/10.1016/j.jastp.2017.07.023>.
- 575 Rodger, C. J., Brundell, J. B., Dowden, R. L., & Thomson, N. R. (2004). Location accuracy of long distance VLF lightning location network. *Annales Geophysicae*, *22*(3), 747–758. <https://doi.org/10.5194/angeo-22-747-2004>.
- Rycroft, M. J., Israelsson, S., and Price, C. (2000), The global atmospheric electric circuit, Solar activity and climate change, *J. Atmos. Sol. Terr. Phys.*, *62*, 1563–1576, [https://doi.org/10.1016/S1364-6826\(00\)00112-7](https://doi.org/10.1016/S1364-6826(00)00112-7)
- 580 Salminen, A., Asikainen, T., Maliniemi, V. & Mursula, K. (2019). Effect of energetic electron precipitation on the northern polar vortex: Explaining the QBO modulation via control of meridional circulation, *Journal of Geophysical Research: Atmospheres*, *124*, 5807–5821

- 585 Satori, G., Williams, E., and Mushtak, V. (2005). Response of the Earth-Ionosphere Cavity Resonator to the 11-year Solar Cycle in X-Radiation, *J. Atmos. Sol. Terr. Phys.*, *67* (6), 553–562.
doi:10.1016/j.jastp.2004.12.006
- Sauvaud, J. A., R. Maggiolo, C. Jacquey, M. Parrot, J. J. Berthelier, R. J. Gamble, and C. J. Rodger (2008), Radiation belt electron precipitation due to VLF transmitters: Satellite
590 observations, *Geophys. Res. Lett.*, **35**, L09101, doi:10.1029/2008GL033194
- Schlegel, K., Diendorfer, G., Thern, S., and Schmidt, M. (2001), Thunderstorms, lightning and solar activity—Middle Europe, *J. Atmos. Sol. Terr. Phys.*, *63*, 1705–1713, doi:10.1016/S1364-6826(01)00053-0.
- Scott, C. J., Harrison, R. G., Owens, M. J., Lockwood, M., and Barnard, L. (2014), Evidence for solar
595 wind modulation of lightning, *Environ. Res. Lett.*, *9*(5), 055004, doi:10.1088/1748-9326/9/5/055004.
- Seppala, A., Randall, C. E., Clilverd, M. A., Rozanov, E., and Rodger, C. J. (2009). Geomagnetic activity and polar surface air temperature variability, *J. Geophys. Res.-Space*, *114*, A10312,
https://doi.org/10.1029/2008JA014029
- Seppala, A., Lu, H., Clilverd, M.A. & Rodger, C.J. (2013). Geomagnetic activity signatures in wintertime
600 stratosphere wind, temperature, and wave response, *J. Geophys. Res. Atmos.*, *118*, 2169-2183
- Shao, X. M., Ho, C., Bowers, G., Blaine, W., and Dingus, B. (2020). Lightning Interferometry Uncertainty, Beam Steering Interferometry, and Evidence of Lightning Being Ignited by a Cosmic ray Shower. *J. Geophys. Res. Atmos.* *125*, e2019JD032273. doi:10.1029/2019JD032273
- Svensmark, H., Bondo, T., and Svensmark, J. (2009). Cosmic ray Decreases Affect Atmospheric
605 Aerosols and Clouds. *Geophys. Res. Lett.* *36*, L15101. doi:10.1029/2009GL038429
- Stringfellow, M. F. (1974), Lightning incidence in Britain and the solar cycle, *Nature*, *249*, 332–333, doi:10.1038/249332a0.
- Sinnhuber, M., Berger, U., Funke, B., Nieder, H., Reddmann, T., Stiller, G., Versick, S., von Clarmann, T., and Wissing, J. M. (2018). NO_y production, ozone loss and changes in net radiative heating due to
610 energetic particle precipitation in 2002–2010, *Atmos.Chem. Phys.*, *18*, 1115–1147,
https://doi.org/10.5194/acp-18-1115-2018, 2018.
- Usoskin, I.G., Kananen, H., Mursula, K., Tanskanen, P., Kovaltsov, G.A. (1998), Correlative study of solar activity and cosmic ray intensity. *J. Geophys. Res.* *103*(A5), 9567,
https://doi.org/10.1029/97JA03782
- 615 Virts, K. S., Wallace, J. M., Hutchins, M. L., & Holzworth, R. H. (2013). A new ground-based, hourly global lightning climatology, *Bulletin of the American Meteorological Society (AMS)*, *94*(9), 1831–1891.

- Voiculescu, M., Usoskin, I., and Condurache-Bota, S. (2013). Clouds Blown by the Solar Wind. *Environ. Res. Lett.* 8, 045032. doi:10.1088/1748-9326/8/4/045032
- 620 Voiculescu, M., and Usoskin, I. (2012). Persistent Solar Signatures in Cloud Cover: Spatial and Temporal Analysis. *Environ. Res. Lett.* 7, 044004. doi:10.1088/17489326/7/4/044004
- Williams, E., Bozóki, T., Sători, G., Price, C., Steinbach, P., Guha, A., Liu, Y., Beggan, C. D., Neska, M., Boldi, R., and Atkinson, M. (2021), Evolution of global lightning in the transition from cold to warm phase preceding two super El Niño events, *J. Geophys. Res.-Atmos.*, 126, e2020JD033526, 625 <https://doi.org/10.1029/2020JD033526>